

GA-A23830

RECENT PROGRESS FROM THE DIII-D PROGRAM

by
A.G. KELLMAN and the DIII-D TEAM

APRIL 2002

DISCLAIMER

This report was prepared as an account of work sponsored by an agency of the United States Government. Neither the United States Government nor any agency thereof, nor any of their employees, makes any warranty, express or implied, or assumes any legal liability or responsibility for the accuracy, completeness, or usefulness of any information, apparatus, product, or process disclosed, or represents that its use would not infringe privately owned rights. Reference herein to any specific commercial product, process, or service by trade name, trademark, manufacturer, or otherwise, does not necessarily constitute or imply its endorsement, recommendation, or favoring by the United States Government or any agency thereof. The views and opinions of authors expressed herein do not necessarily state or reflect those of the United States Government or any agency thereof.

GA-A23830

RECENT PROGRESS FROM THE DIII-D PROGRAM

by
A.G. KELLMAN and the DIII-D TEAM

This is a preprint of a paper presented at the 19th IEEE/NPSS Symposium on Fusion Engineering, January 21-25, 2002 in Atlantic City, New Jersey and to be published in the *Proceedings*.

Work supported by
the U.S. Department of Energy under
Contract No. DE-AC03-99ER54463

GA PROJECT 30033
APRIL 2002

Recent Progress From the DIII-D Program

A.G. Kellman and the DIII-D Team

General Atomics, P.O.Box 85608, San Diego, California 92186-5608

Abstract—Significant progress has been made in a number of key scientific and engineering areas that are critical to advanced tokamak operation on the DIII-D tokamak. Improved error field correction coupled with plasma rotation has resulted in a passive wall stabilized discharge at twice the no-wall beta limit. Active feedback stabilization of the resistive wall mode (RWM) has been improved using newly installed internal magnetic sensors and external control coils. A set of internal control coils for RWM feedback has been designed that should permit operation at close to the ideal limit. Real-time stabilization of the neoclassical tearing mode has been achieved using a new “search and suppress” control algorithm coupled with electron cyclotron current drive (ECCD). The ECCD system is routinely providing in excess of 2 MW of power for 2 s pulses. Modeling predicts that measured efficiencies of ECCD are consistent with future, fully non-inductive AT target discharges. Massive injection of argon gas has resulted in successful mitigation of disruptions in high performance discharges without producing high energy runaway electrons. Finally, an upgraded digital plasma control system will provide significantly more capability to provide real time measurement and control of plasma profiles and instabilities.

I. INTRODUCTION

Design of conventional tokamaks is focussed around moderate values of plasma confinement, $H < 2$ ($H = \tau_E / \tau_{ITER89P}$), and plasma stability, $\beta_N < 2.5$ [$\beta_N = \beta / (I/aB)$] with high power rf and/or neutral beam heating proposed to achieve steady state operation. A figure of merit often used to characterize progress toward an advanced tokamak (AT) is the product $\beta_N H$. A high value permits a compact device with high fusion power density, fusion gain, and low current drive power requirements. To enhance the commercial attractiveness of the tokamak relative to a conventional design, the DIII-D program is focussing on developing the scientific basis for advanced modes of tokamak operation. This advanced tokamak is envisioned as a more compact, highly shaped plasma operating at higher β_N (approaching 5), higher confinement (H approaching 3), with no inductive current drive, and low recirculating power. The high stability and confinement require the use of both current and pressure profile control and an active feedback system for control of plasma instabilities. The latter two conditions require a steady-state current drive and a high bootstrap current fraction to reduce the power requirements for the current drive system. Recent engineering and scientific advances from the DIII-D program have permitted significant progress toward these high performance and steady-state goals. While there are many different approaches to achieve advanced performance plasmas, much of the recent research on DIII-D has focussed on two approaches. Our highest

performance is achieved in H-mode discharges with negative magnetic shear in the plasma core, broad pressure profiles, and high shear in the rotation profile which suppresses turbulence induced transport [1,2,3]. A second approach, known as Quiescent Double Barrier mode (QDB) [4,5,6] is produced using counter-injected neutral beam heating and combines an internal transport barrier with a quiescent, H-mode edge transport barrier, i.e. it does not have the undesirable pulsed heat loads associated with edge localized modes that a standard H-mode discharge exhibits. Highlights of the recent program results discussed in this paper include: stabilization of performance limiting plasma instabilities using rotation, magnetic and rf techniques, higher power and longer pulse rf heating and current drive system development, improved performance and characterization of QDB discharges, successful demonstration of a technique for mitigation of disruptions of high performance discharges, and an upgrade to the digital plasma control system.

II. RECENT PROGRESS

High performance AT discharges in DIII-D are characterized by high $\beta_N H$ product and high T_E in order to maximize current drive efficiency. Operation in this regime is limited by two plasma instabilities, the resistive wall mode (RWM) and the neoclassical tearing mode (NTM). In the absence of a conducting wall surrounding the plasma, the beta is limited by an $n=1$ external kink at a value of β_N (no wall). The presence of an ideal conducting wall immediately surrounding the plasma results in a significantly higher beta limit, β_N (ideal). In the presence of a resistive wall, the $n=1$ ideal kink is manifested as a resistive wall mode and can again grow. Like the ideal kink, the mode causes a significant loss of plasma thermal energy and may lead to a disruption. Two techniques have been studied on DIII-D to address the RWM: wall stabilization by plasma rotation and active feedback control. Effective wall stabilization has been achieved by rotating the plasma with high power neutral beams and significantly reducing the magnetic error fields that produce magnetic drag and reduce the rotation speed [7,8]. Experiments conducted this year showed that as β_N increases above β_N (no wall), the plasma amplifies the effect of the intrinsic magnetic error fields which in turn reduces the rotation. When the rotation falls below a critical value, the RWM becomes unstable (Fig. 1). In the wall stabilization experiments, the error correction was achieved using the set of six external picture frame coils (C-coil) on the vessel midplane. By optimizing the error field correction, plasma rotation has been maintained and it has been demonstrated that the RWM can be stabilized up to approximately twice the no wall beta limit and to near the ideal wall limit. In our highest performance discharge, we have $\beta_N \sim 6\ell_i$ for $4\tau_E$ limited only

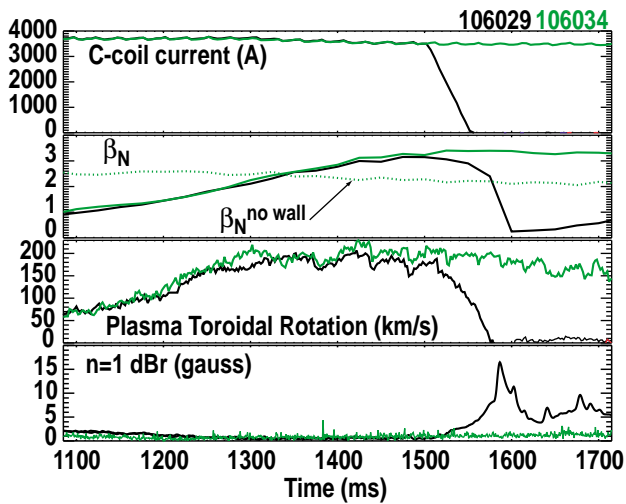


Fig. 1. For $\beta_N > \beta_{N(\text{no wall})}$, if the C-coil error correction current is turned off, plasma rotation slows down and the $n=1$ external kink mode grows. If optimized error correction is maintained, plasma rotation remains high and provides wall stabilization of the $n=1$ external kink.

by the onset of a $m=2, n=1$ tearing mode. This value of beta is 50% above the no-wall beta limit. Long pulse, wall stabilized discharges have also been maintained with a volume averaged $\beta > 3\%$ for a duration $\sim 10 \tau_E$. These high fusion performance levels are sustained with a broad current profile having $\ell_1 \sim 0.7$, and relatively flat q -profile ($q_{\min} > 1.5$ and $q_{95} < 4$), resulting in a plasma that would be highly unstable without the effect of a surrounding conducting wall. [7].

While wall stabilization due to plasma rotation is effective on DIII-D, devices with little or no momentum input may not have sufficient rotation to stabilize the RWM. Calculations using the VALEN code [9] show that feedback control of the RWM using the external C-coils can effectively stabilize the mode significantly above the no-wall limit even without rotation (Fig. 2). Recent experiments using newly installed internal sensor loops (to measure δB_r) and discrete Mirnov coils (to measure δB_{pol}) have qualitatively confirmed the prediction of the VALEN code. $\beta_N > \beta_{N(\text{no wall})}$ is obtained with active feedback control of the RWM and the improvement in β_N increases as the sensor coils are changed from the external δB_r loops, to internal δB_r loops, to internal δB_{pol} probes [10].

To further increase the achievable β_N , we are proceeding with the design and installation of internal control coils. VALEN3D predicts that the addition of 12 internal control coils (six above and six below the vessel midplane) can stabilize β_N values up to 97% of the difference between the no wall and the ideal wall limit (Fig. 2). No significant improvement in β_N can be achieved by adding six additional internal coils on the midplane since the off-midplane coils are well matched to the RWM structure. Error field correction will be provided by the existing external C-coil and the internal coils will provide the active feedback control of the RWM. Each internal coil will consist of a single turn of a water cooled copper conductor. The copper is insulated from the vessel with a high temperature polyimide, Vespel and

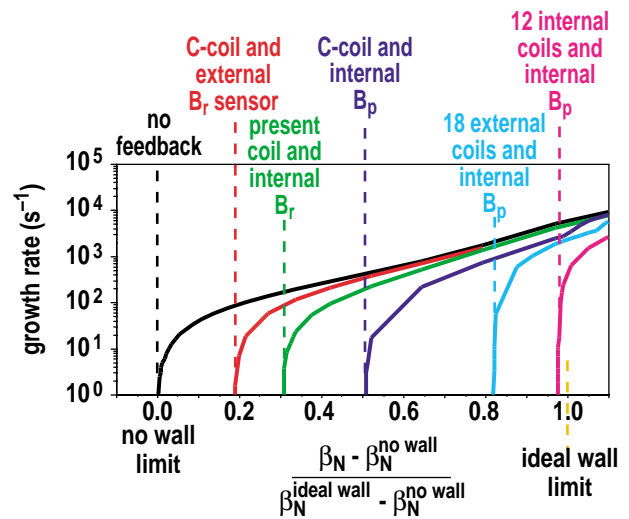


Fig. 2. VALEN3D predicts improved feedback stabilization of RWM with internal B_{pol} sensors compared to either external or internal B_r sensors. Calculations also show the improvement expected with an 18 external coil set and the proposed 12 internal coil set. The new internal coil set should permit operation close to the ideal wall limit.

Kapton® sheets (to increase tracking length) and has been tested to 4 kV. The copper/insulator combination is isolated from primary vacuum by being enclosed in a stainless steel tube that mounts directly to the vessel wall behind the graphite armor tiles (Fig. 3). The coil leads were designed to be coaxial to eliminate any error fields. The advantages of the internal coil system relative to the existing external coils include: (1) the harmonic spectrum of the internal coils above and below the midplane is better matched to the RWM ($m \sim 3-5$), (2) the closer proximity of the coils to the plasma allows a 7 kA single turn to produce $\sim 20\%$ more field at the plasma edge than the existing four turn, 20 kA-turn external coil, and (3) the lower inductance internal coil will have significantly higher bandwidth ($dI/dt \sim 5-10$ times higher than the external C-coil with the same supply). Comparison of internal versus external off-midplane coils show that the field produced at the plasma edge at 1 kHz (normalized by the DC value) is ~ 3 times higher for the internal coil set because of the reduced shielding effect of the wall. The first two coils were installed in Fall 2001 and have been successfully baked to 350°C and operated to ~ 5 kA. The full 12 coil set will be installed in Fall 2002.

Significant progress has also been made in the stabilization of the neoclassical tearing mode. Theory predicts that by using electron cyclotron current drive (ECCD) to replace the missing bootstrap current in the O-point of the island of the NTM, the mode should be stabilized. This was demonstrated in proof-of-principle experiments in which a saturated $m=3, n=2$ NTM was fully suppressed using 2.3 MW of ECCD for 1 s [11]. By moving the plasma on a shot-by-shot basis, the rf power was directed off-axis to be coincident with the $q=3/2$ surface. We have now implemented real-time NTM suppression by moving the plasma radially until the off-axis ECCD coincides with the island [11-13]. This is done

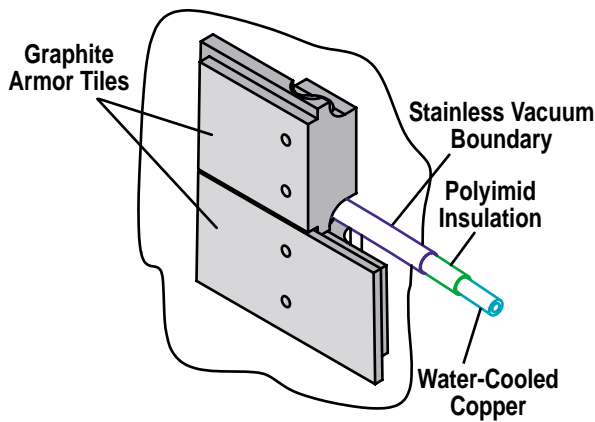


Fig. 3. New internal RWM control coils consist of a set of 12 single turn, actively water-cooled, copper loops. The coils will be located above and below the midplane and behind the protective armor tiles.

using a blind search and suppress algorithm initiated whenever the 3/2 amplitude exceeds a threshold value. The plasma is moved rigidly by ~ 1 cm with dwell time in each radial position of 50–100 ms (Fig. 4). The search continues until the mode is suppressed below the threshold. A similar suppression was also performed by varying the toroidal field in 0.01 T steps to move the resonant location instead of the radial position. A new ECH launcher designed by PPPL will permit real time poloidal and toroidal steering of the ECH which should permit a more direct mode suppression technique. Fig. 5 shows that following the successful suppression of a 3/2 NTM using 2.3 MW of ECCD the plasma β_N was increased by 50% from 2 to 3 without the reappearance of the mode. Attempts to stabilize the 2/1 NTM in our highest performance AT discharges using 2.5 MW of ECCD has resulted in only partial suppression of the mode. These experiments will be repeated this coming year with the higher power we expect from the ECCD system.

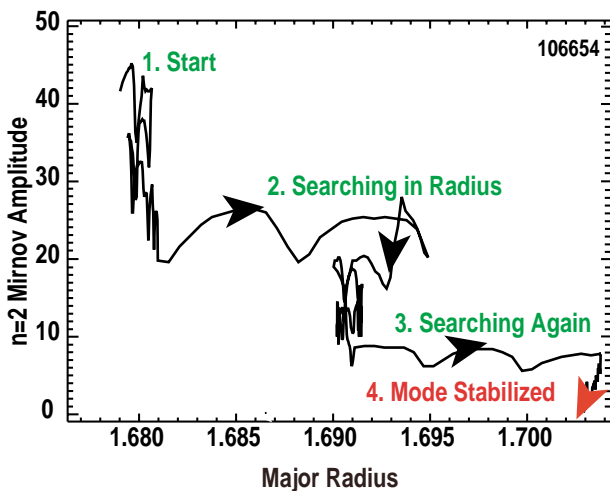


Fig. 4. In the “search and suppress” algorithm, the plasma control system moves the plasma radial position in 1 cm increments, testing to see if the amplitude of the $n=2$ mode decreases at the new position. The search continues until the mode amplitude is below a threshold value. The direction of plasma movement is reversed if the mode amplitude increases.

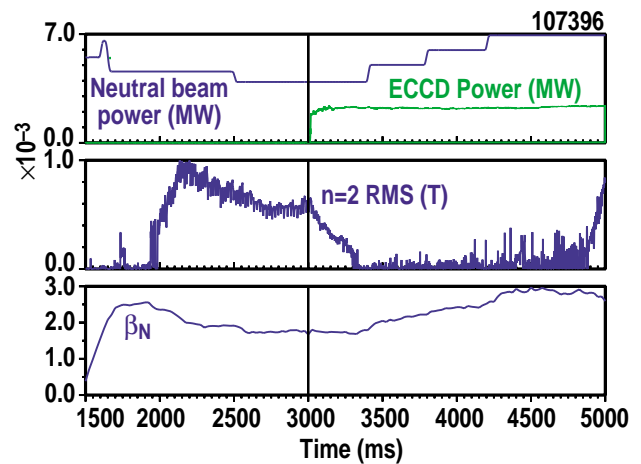


Fig. 5. A 3/2 neoclassical tearing mode (NTM) onsets at $t \sim 1900$ ms, at a value of $\beta_N \sim 2.5$ resulting in a decrease in the β_N . Complete stabilization of the NTM is achieved approximately 600 ms after the onset of ECCD. β_N is subsequently increased by 50% without the reappearance of the mode.

A key element of the advanced tokamak program is electron cyclotron current drive. This current drive technique is required for steady-state current drive, current profile shaping to enlarge the stable operating space, and active feedback control of the neoclassical tearing mode. Progress has been made both in the system hardware and in the theoretical understanding of ECCD.

Completion of a third mod/reg power supply and improvements in the reliability of the existing hardware resulted in a 90% reliability for the 4 gyrotron system by the end of this operating year [14]. The 4 gyrotrons routinely deliver 2.3 MW of EC power for 2 s pulses. Three of the gyrotrons are manufactured by GYCOM and are rated for 2 s pulses and the fourth, manufactured by Communication Power Industries (CPI) with a CVD diamond window is rated at 1 MW for 10 s. Worldwide, several CVD diamond windows on long pulse gyrotrons have failed due to braze failures or broken windows due to contamination that occurred during brazing [15]. Raman scattering measurements verified the presence of graphite contamination and IR measurements on a window installed on the gyrotron identified hot spots on the window during operation. Following grit blasting of the window, the graphite was removed and most of the hot spots were eliminated. We believe that the present gold braze with improved assembly and brazing technique will provide robust operation for 10 s at 1 MW. Operation of the gyrotron at 1 MW for 5 s has recently been demonstrated into a compact dummy load at GA [16] and *in situ* IR camera measurements on the diamond window indicate that the present CPI gyrotron can safely go to full power and pulse length. Two additional 10 s, 1 MW gyrotrons should be available this coming year bringing the source power to 5.1 MW with 75%–80% of the power delivered to the plasma. The system has six launchers with poloidal sweeping capability, and two of these designed by PPPL can also sweep toroidally from co- to counter-current drive. A newly designed mirror has now extended the pulse duration of the poloidal-only sweep launchers to 10 s [17].

The most significant result in the understanding of ECCD has been in the role of particle trapping. In earlier experiments performed at low beta [18], the efficiency for off-axis ECCD was well below that required for our AT discharges. Theoretical modeling [19] has shown and is now confirmed by recent experiments [20] that as the electron beta is increased, the coupling of the applied rf power to trapped electrons (which do not contribute to plasma current) is reduced. Thus, in the regimes of higher beta relevant to our AT discharges, the measured and predicted current drive efficiency is significantly higher (Fig. 6) [1]. The achievement of a fully non-inductive 650 kA discharge with higher electron beta again confirmed the higher ECCD efficiency, $(I/P)_{\text{ECCD}} \sim 36 \text{ kA/MW}$, and will permit the study of discharges with high bootstrap fraction ($>70\%$). Modeling of a target AT discharge ($\beta_N = 4$, $H=3$, $I_p=1.2 \text{ MA}$) with 3.5 MW of ECCD and 7.9 MW of neutral beam injection yields an even higher efficiency ($I/P = 46 \text{ kA/MW}$) and shows that a fully non-inductive AT discharge can be obtained [21].

The previous discussions have focussed on individual elements that are key to steady state AT discharges. However, significant progress has also been made in the demonstration of a discharge that integrates many of the elements of AT operation. By combining the rotational stabilization of the RWM with an internal transport barrier and a weakly negative central shear profile, DIII-D has sustained a value of $\beta_{NH} > 12$ for $5 \tau_E$ with approximately 65% bootstrap fraction and a non-inductive current fraction of 85% [1] (Fig. 7). This is above the design value of $\beta_{NH} \sim 11$ for the ARIES-RS. These discharges also demonstrated that density control could be obtained in an AT shape and the current drive efficiency was consistent with predictions.

Although not exhibiting the highest performance, progress continues to be made in the performance, modeling, and the control of the Quiescent Double Barrier mode (QDB) discharges [4-6]. These discharges possess both internal and

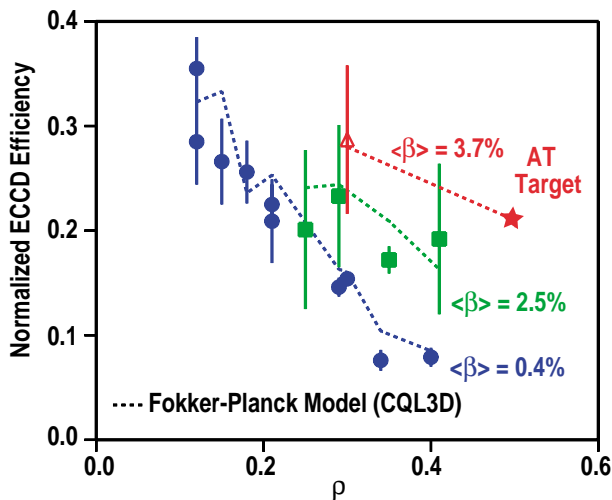


Fig. 6. At low β_e , normalized ECCD efficiency decreases at larger heating radii because of strong coupling of the rf power to trapped electrons. At higher values of β_e , the trapping effect is reduced and the efficiency is sufficient for our needs for our AT target discharge.

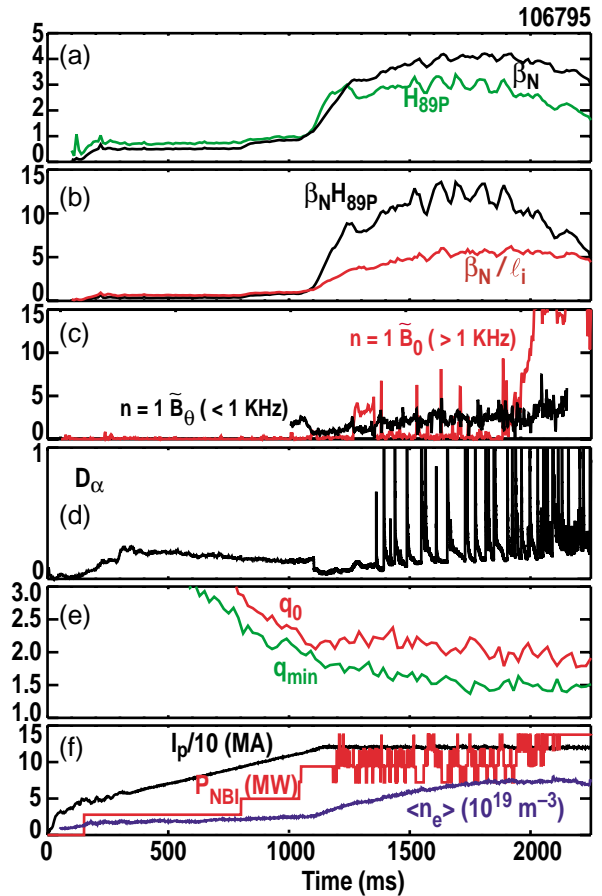


Fig. 7. A fully wall stabilized discharge, with an internal transport barrier and weakly negative central shear has been achieved with $\beta_N H > 12$ for $5 \tau_E$. (a) $\beta_N \sim 4$ and $H_{89P} \sim 3$; (b) $\beta_N H_{89P} \sim 12$ and $\beta_N / \ell_i \sim 6$ about 50% above the no-wall limit; (c) rotation stabilizes the low frequency RWM, but a 2/1 tearing mode grows at $\sim 1900 \text{ ms}$; (d) D_α showing ELMy H-mode during high performance phase; (e) minimum safety factor, q_{min} , is maintained above 1.5 throughout the high performance phase with the central q near 2; (f) plasma current, I_p , injection neutral beam power, P_{NBI} , and line averaged density, $\langle n_e \rangle$.

edge transport barriers in both the electron and ion channels, however, the high pulsed, power loads associated with ELMs in H-mode are replaced by a coherent MHD mode, referred to as the edge harmonic oscillation (EHO). The EHOs, enhance particle transport through the plasma boundary resulting in good density and radiated power control, and allow large pedestal temperatures to be maintained, without the detrimental effects of large ELMs. Production of the QDB requires sufficient counter- neutral beam injection, good divertor pumping, and a large plasma-wall gap on the low field side. The mode has been obtained over a wide range of triangularity ($0.16 < \delta < 0.7$) and moderate values of safety factor ($3.7 < q < 4.6$). Values of $\beta_{NH} \sim 7$ have been maintained for $10\tau_E$ and the mode has been maintained for 3.5 s or $25\tau_E$ limited only by the duration of the neutral beam pulses. In the plasma core, simulations replicate many of the observed features of the turbulence; in particular that the turbulence is not fully suppressed as is normal for

internal transport barriers in DIII-D. Despite the incomplete turbulence suppression, core transport in the QDB is very small, which may be explained by shorter turbulence correlation lengths in these discharges [22]. The peaked density and pressure profiles in these discharges, however, lead to lower beta limits, non-optimal bootstrap current profiles [23], and slow high-Z impurity accumulation in the plasma core [24]. A number of control techniques have been investigated with some success at reducing the central density: near on-axis ECH, off-axis pellet injection, increased discharge triangularity, and impurity puffing [25].

Despite considerable improvements in our ability to avoid or to actively control plasma instabilities in high performance discharges, even infrequent disruptions in a high current, high energy density tokamak reactor can result in unacceptable damage to the vessel or its internal components via erosion or melting of the first wall, impact by runaway electrons produced during the disruption, or electromagnetic loads caused by eddy currents or halo currents. A successful and robust technique for mitigation of disruptions in these discharges is essential for the realization of the tokamak as a reactor. By using a fast acting valve to inject $\sim 4 \times 10^{22}$ atoms of Ar, a successful mitigation technique has been demonstrated on DIII-D AT discharges [26,27]. This massive gas puff quickly drops the electron temperature to 1–2 eV which results in a rapid current decay, reduced halo currents, and radiation of $\sim 99\%$ of the thermal and magnetic energy without the production of high energy runaway electrons. The massive gas puff is found to penetrate into the plasma center at approximately the sonic speed (~ 250 m/s for Ar) for all gases tested (D_2 , He, Ne, and Ar) because the pressure of the gas jet exceeds that of the plasma. While the radiation from the impurity ions rapidly radiates the stored energy, it also produces a low electron temperature and a thus a low effective charge state ($Z_{\text{eff}} \sim 1$). This low charge state coupled with the extremely high density of the high Z injected neutral impurity gas inhibits the generation and amplification of runaway electrons. Unlike the injection of high Z solid pellets which results in significantly lower density of impurity atoms, the gas technique does not produce runaways (Fig. 8). The high pressure gas jet technique is simple and scales favorably to a reactor class tokamak.

A critical element to the success of the DIII-D physics research program has been capability to flexibly implement the many required control schemes. This is provided by the DIII-D digital plasma control system (PCS) [28–30]. The PCS collects 232 analog and digital diagnostic signals and processes these data in real time on multiple processors executing in parallel. For a control algorithm that requires relatively high frequency response, a processor can be dedicated to that single algorithm. This is the case for both the vertical position control and the resistive wall mode control algorithms which update power supply demand signals at approximately 16 kHz and 7 kHz respectively. Other control applications, such as discharge shape control, require substantial processing power and so are implemented using

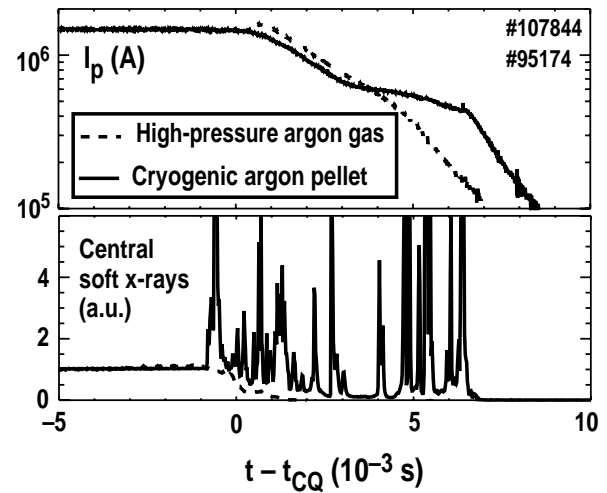


Fig. 8. Injection of high pressure Ar gas results in rapid discharge termination (shot #107844) without the generation of a runaway electron tail as observed with solid cryogenic Ar pellet injection (shot #95174).

multiple processors. Shape control is implemented on 3 processors using the isoflux method [31] and a real time implementation of the EFIT equilibrium reconstruction calculation.

A major upgrade of the processing power and flexibility of the PCS is in progress in order to provide the capability to satisfy the future requirements for advanced tokamak discharges such as current and profile control. The 40 MHz processors presently in use are being replaced by a mixture of Alpha and Pentium 4 processors with 10–40 times more processing power, the improvement depending on the algorithm [32]. In addition, the new processors use the PCI bus for expansion rather than the VME bus. This allows flexibility in the choice of processor and data acquisition. In the present PCS, there is a proprietary interface between the processor and data acquisition that limits the ability to change the processor [33]. In the upgraded PCS, analog data acquisition uses 32 channel PCI bus digitizers with 16 bit simultaneous sampling. Specialized firmware in the digitizer provides low latency transfers of the data to the processor with less than $8 \mu\text{s}$ delay between the digitizer trigger and data arriving in processor memory. The processors in the new PCS are connected by a Myrinet switched network that provides 2 Gbit/s, low latency ($8 \mu\text{s}$), real time communication. The Myrinet network can be implemented using optical fiber providing the capability to locate PCS processors and data acquisition in remote parts of the laboratory where diagnostics such as Thomson scattering and charge exchange recombination are located. This flexibility will allow the future addition to the PCS of diagnostics required for pressure or rotation profile control. One of the first new applications of the enhanced capability in the PCS-upgrade will be the use of data from the motional Stark effect diagnostic measurement of magnetic field pitch angles in the real time equilibrium reconstruction to obtain the safety factor profile. This analysis can be used to implement control of the current or safety

factor profile and to identify the location of the 3/2 safety factor surface to aid in the NTM suppression.

III. SUMMARY

Significant progress has been made in obtaining and sustaining enhanced performance discharges in DIII-D. Different control methods, both passive and active have been explored in the control of performance limiting plasma instabilities. Higher power and longer pulse length on the ECCD system (expected in early 2002) and a new set of 12 internal control coils for active RWM feedback control (expected in early 2003) should further extend the ability to sustain AT discharges. Improved density control or other technique for increasing the electron temperature is a critical need in order to achieve sufficient current drive for fully non-inductive AT discharges. Development of a successful and robust disruption mitigation technique on DIII-D has removed a significant obstacle to the realization of a commercially viable tokamak reactor.

ACKNOWLEDGEMENT

Work supported by U.S. Department of Energy under Contract No. DE-AC03-99ER54463.

REFERENCES

- [1] M.R.Wade, et al., "Physics of High Bootstrap Fraction, High Performance Plasmas on DIII-D Tokamak", Proc.28th EPS Conf. on Controlled Fusion and Plasma Physics, Madeira, Portugal, 2001, to be published.
- [2] C.M. Greenfield, et al., Physics of Plasmas **7**, 1959 (2000).
- [3] K.H. Burrell, Physics of Plasmas **6**,4418 (1999).
- [4] K.H. Burrell, Physics of Plasmas **8**, 2153 (2001).
- [5] C.M. Greenfield et al., Phys.Rev.Letters **86**,4544 (2001).
- [6] E.J. Doyle, et al. "Progress Towards Increased Understanding and Control of Internal Transport Barriers on DIII-D," Proc. 18th IAEA Fusion Energy Conference, Sorrento, Italy, 2000 (IAEA, Vienna), to be published.
- [7] A.M. Garofalo, et al., "Sustained Stabilization of the Resistive Wall Mode by Plasma Rotation in DIII-D," submitted to Phys. Rev. Let.
- [8] A.M. Garofalo, "Sustained Rotational Stabilization of DIII-D Plasmas Above the No-Wall Limit," accepted for publication in Physics of Plasmas.
- [9] J. Bialek, et al., Physics of Plasmas **8**, 2170 (2001).
- [10] L.C. Johnson, et al., "Structure and Feedback Stabilization of the Resistive Wall Mode in DIII-D," Proc. 28th EPS Conf. on Controlled Fusion and Plasma Physics, Madeira, Portugal, 2001, to be published.
- [11] R.J. La Haye, et al., "Suppression of Neoclassical Tearing Modes in the Presence of Sawteeth Instabilities by Radially Localized Off-axis Electron Cyclotron Current Drive in the DIII-D Tokamak," Proc. 28th EPS Conf. on Controlled Fusion and Plasma Physics, Madeira, Portugal, 2001, to be published.
- [12] R.J. LaHaye et al., "Control of Neoclassical Tearing Modes in DIII-D," accepted for publication in Physics of Plasmas.
- [13] D.A. Humphreys, et al., "Design, Simulation, and Operational Use of Control Algorithms for ECCD Suppression of the m/n=3/2 Neoclassical Tearing Mode," Bull. Am. Phys. Soc. **46**, 299 (2001).
- [14] J.M. Lohr, et al., "ECH Comes of Age for Magnetic Fusion Research," these proceedings.
- [15] I.A. Gorelov, et al., "Infrared Measurements of the Synthetic Diamond Window in a 110 GHz High Power Gyrotron," Proc. 14th Topical Conference on Radio Frequency Power in Plasmas, Oxnard, California, 2001, to be published.
- [16] J.L. Doane, Int. Jour. of Infrared and Millimeter Waves **14**,363 (1993).
- [17] C.B. Baxi, M.E. Friend, J.L. Doane, E.E. Reis, and R.W. Callis, "Thermal Design of GA ECH Launcher Mirror for Long Pulse Operation," these proceedings.
- [18] T.C. Luce, et al., Phys. Rev. Letters **83**,4550 (1999).
- [19] R. Prater, et al., "Decrease in Trapping Effects for Off-Axis Electron Cyclotron Current Drive in High Performance Plasmas," Proc. 14th Topical Conference on Radio Frequency Power in Plasmas, Oxnard, California, 2001, to be published.
- [20] C.C. Petty, et al., "Electron Cyclotron Wave Experiments on DIII-D," Proc. 14th Topical Conference on Radio Frequency Power in Plasmas, Oxnard, California, 2001, to be published.
- [21] M. Murakami, et al., "Advanced Tokamak Scenario Modeling Using Electron Cyclotron Current Drive in DIII-D," Bull. Am. Phys. Soc. **46**, 299 (2001).
- [22] C.M. Greenfield, et al., "The Quiescent Double Barrier Regime in DIII-D," to be published in Plasma Physics and Controlled Fusion (2992).
- [23] W.A. Houlberg, et al., Physics of Plasmas **4**, 3230 (1997).
- [24] W.P. West, "Energy, Impurity and Particle Transport in Quiescent Double Barrier Discharges in DIII-D," accepted for publication in Physics of Plasmas.
- [25] E.J. Doyle, et al., "Recent Results from Quiescent Double Barrier Regime on DIII-D," Bull. Am. Phys. Soc. **46**, 299 (2001).
- [26] P.L. Taylor, et al., Physics of Plasmas **6**,1872 (1999).
- [27] D.G. Whyte, et al., "Mitigation of Tokamak Disruptions Using High-Pressure Gas Injection," submitted to Phys. Rev. Letter.
- [28] G.L. Campbell, et al., Proc. 17th Symp. on Fusion Technology, Rome, Italy (Elsevier Scientific Publishers, B.V. 1993) 1017.
- [29] M.L. Walker, et al., Proc. 16th IEEE/NPSS Symp. on Fusion Engineering, September 30–October 5, 1995, Champaign, Illinois, Vol. 2, p. 885 (Institute of Electrical and Electronics Engineers, Inc., Piscataway, New Jersey) (1996).
- [30] J.R. Ferron, et al., Proc. 16th IEEE/NPSS Symp. on Fusion Engineering, September 30–October 5, 1995, Champaign, Illinois, Vol. 2, p. 870 (Institute of Electrical and Electronics Engineers, Inc., Piscataway, New Jersey) (1996).
- [31] J.R. Ferron, et al., Nucl. Fusion **38**, 1055 (1998).
- [32] B.G. Penaflor, et al., Proc. 21st Symp. on Fusion Technology, Madrid, Spain (2000) to be published.
- [33] J.R. Ferron, et al., Rev. Sci. Instr. **63**, 5464 (1992).